

**\*\*FULL TITLE\*\***  
*ASP Conference Series, Vol. \*\*VOLUME\*\*, \*\*YEAR OF PUBLICATION\*\**  
**\*\*NAMES OF EDITORS\*\***

## The small-scale solar surface dynamo

Jonathan Pietarila Graham, Sanja Danilovic, and Manfred Schüssler

*Max-Planck-Institut für Sonnensystemforschung, 37191  
 Katlenburg-Lindau, Germany*

**Abstract.** The existence of a turbulent small-scale solar surface dynamo is likely, considering existing numerical and laboratory experiments, as well as comparisons of a small-scale dynamo in MURaM simulations with *Hinode* observations. We find the observed peaked probability distribution function (PDF) from Stokes- $V$  magnetograms is consistent with a monotonic PDF of the actual vertical field strength. The cancellation function of the vertical flux density from a *Hinode* SP observation is found to follow a self-similar power law over two decades in length scales down to the  $\approx 200$  km resolution limit. This provides observational evidence that the scales of magnetic structuring in the photosphere extend at least down to 20 km. From the power law, we determine a lower bound for the true quiet-Sun mean vertical unsigned flux density of  $\approx 43$  G, consistent with our numerically-based estimates that 80% or more of the vertical unsigned flux should be invisible to Stokes- $V$  observations at a resolution of 200 km owing to cancellation. Our estimates significantly reduce the order-of-magnitude discrepancy between Zeeman- and Hanle-based estimates.

### 1. Introduction

The existence of a global solar dynamo is generally accepted, though it is not well understood. There is evidence for a second, local dynamo operating near the solar surface – the so-called solar-surface dynamo (Petrovay & Szakaly 1993).<sup>1</sup> This dynamo may be driven by turbulence: magnetic energy is amplified by random stretching of magnetic field lines by turbulent motions (Batchelor 1950). Magnetic energy is lost to Ohmic dissipation. For dynamo action to succeed, stretching must dominate over dissipation. The relative strengths of these two effects is quantified by the magnetic Reynolds number,  $Re_M \equiv v_0 l_0 / \eta$  ( $v_0$  and  $l_0$  are typical velocity and length scales and  $\eta$  the magnetic diffusivity). Similarly, the kinetic Reynolds number is  $Re \equiv v_0 l_0 / \nu$  where  $\nu$  is the kinematic viscosity. When  $Re_M$  exceeds a critical threshold,  $Re_M > Re_M^C$ , dynamo action results.

Two different types of dynamo can be found, depending on the presence or absence of net flow helicity (Meneguzzi et al. 1981). With net helicity, magnetic energy grows at scales larger than the energy-containing scale of the fluid motions: large-scale dynamo (LSD) or mean-field dynamo. LSDs are often studied with mean-field theory; the production of large-scale magnetic energy is approx-

---

<sup>1</sup>Actually, in simulations, turbulent dynamo action occurs in the bulk of the convection zone, though greater than solar rotation rate may be required to generate large-scale field in the absence of shear (Brown et al. 2007).

imately the alpha-effect (see, e.g., Brandenburg 2003). Without net helicity, dynamo action is harder to achieve and magnetic energy grows at scales smaller than the forcing scale. This latter defines small-scale dynamo (SSD) or fluctuation dynamo action. Near the solar surface, the convective time scale is much shorter than the rotation period, the effects of rotation can be neglected, and a flow with no net helicity results. Any surface dynamo will thus be a SSD.

This is also suggested by observation of the small-scale magnetic field in the quiet Sun. In high resolution magnetograms we see mixed polarity fields on small scales, which is variously called the magnetic carpet or the salt-and-pepper pattern (Title & Schrijver 1998; Hagenaar et al. 2003), consistent with the idea of SSD action. As turbulent convection can drive small-scale dynamo action (in numerical simulations of Boussinesq convection without rotation Cattaneo 1999; Cattaneo et al. 2003), observations and simulations together provide evidence of a SSD driven by turbulence at the solar surface (likely deeper as well).

Several arguments can be put forward against a small-scale solar dynamo. Firstly, there exists the possibility that the small-scale field is solely produced by the shredding up of large-scale field by turbulence. However, observationally the amount of small-scale flux is not dependent on the solar cycle (Hagenaar et al. 2003; Trujillo Bueno et al. 2004). This might not be the case if the small-scale flux is the result of the shredding up of the field from the global dynamo. It might also then show some latitudinal dependence (among low latitudes). Assuming the existence of both SSD and shredding, small-scale dynamo is predicted to create small-scale magnetic field at the turbulent rate of stretching ( $\propto Re_M^{1/2}$ , see, e.g., Iskakov et al. 2007) which is much faster either than large-scale field can be produced (at time scales associated with the kinetic-energy-containing length scales) or be shredded up by the turbulence (Schekochihin et al. 2005).

Secondly, small-scale dynamo action may not be possible at the magnetic Prandtl number,  $P_M$ , of the solar plasma,  $P_M \equiv Re_M/Re \approx 10^{-5}$ :  $Re_M^C$  sharply increases with decreasing  $P_M$  (increasing  $Re$ ) since eddies smaller than the characteristic scale of the magnetic field diffuse the field and inhibit dynamo action. The two asymptotic possibilities are  $Re_M^C \rightarrow \text{const}$  as  $Re \rightarrow \infty$  (SSD at low  $P_M$ ; Rogachevskii & Kleeorin 1997; Boldyrev & Cattaneo 2004) or  $Re_M^C/Re = P_M^C \rightarrow \text{const}$  as  $Re \rightarrow \infty$  (no SSD at low  $P_M$ ; Schekochihin et al. 2005). Numerical simulations of low  $P_M$  SSDs have focused on the existence (or not) of a time-averaged mean flow. Such a flow exists for the Sun and many other astrophysical cases. Both with (Ponty et al. 2005) and without a mean flow (Iskakov et al. 2007), a plateau in  $Re_M^C$  was found. This suggests such dynamo action should be possible on the Sun. However, the  $P_M$  of the sun is 3 orders of magnitude smaller than that accessible to present numerical computations; the observed plateaus may not represent the asymptotic behavior. Fortunately, a laboratory dynamo resulting from unconstrained turbulence in liquid sodium ( $P_M \approx 10^{-5}$ ) has been demonstrated (Monchaux et al. 2007) establishing that a turbulent dynamo is possible at values of  $P_M$  corresponding to the solar plasma.

## 2. The MURaM code and the solar surface dynamo

The remaining objection against a surface dynamo was raised by Stein et al. (2003): unlike the Cattaneo (1999) simulation, the Sun is strongly stratified and magnetic flux is swept into the down-flow lanes and subject to long recirculation times. In the simulations of Stein et al. (2003) with open boundaries, no dynamo action was found. However, Vögler & Schüssler (2007) have demonstrated SSD action for sufficiently high  $Re_M$  using the MURaM code (Vögler 2003; Vögler et al. 2005). They simulated a box with strong stratification and open boundaries, but prevented advection of magnetic flux from outside the box: providing an artificially isolated surface layer ignoring any SSD action that may occur in deeper layers. They conducted 3 simulations with increasing  $Re_M$  (see Table 1). Above the critical threshold,  $Re_M^C \sim 2000$ , dynamo action occurs. The magnetic energy spectrum peaks at scales smaller than the energy-containing scale of the fluid motions, demonstrating that SSD is a possibility for a solar surface dynamo despite strong stratification and little recirculation. In Table 1, dynamo action in the 3 MURaM simulations of Vögler & Schüssler (2007) as well as in the simulations of Cattaneo (1999) and of Stein et al. (2003) is indicated solely by their  $Re_M$  and  $P_M$ . For the simulations below the critical threshold for dynamo action, ( $Re_M^C \gtrsim 1000$ ), there is no dynamo action. The result by Cattaneo (1999) is an exception as  $P_M > 1$  and this lowers the threshold.

Table 1. Simulations by Cattaneo (1999), Stein et al. (2003), and Vögler & Schüssler (2007): computational grid size, magnetic Reynolds and Prandtl numbers, boundary conditions (BC; open or closed), and presence of SSD.

Simulation	Grid pts.	$Re_M$	$P_M$	BC	SSD
Run A	$288^2 \times 100$	$\approx 300$	$\lesssim 1$	open	N
Stein et al.	$253^2 \times 163$	$\approx 600$	$\approx 1$	open	N
Run B	$576^2 \times 100$	$\approx 1300$	$\lesssim 1$	open	N
Cattaneo	$512^2 \times 97$	$\approx 1000$	$\approx 5$	closed	Y
Run C	$648^2 \times 140$	$\approx 2600$	$\lesssim 1$	open	Y

The MURaM Run C dynamo also reproduces, quantitatively, some aspects of observations. For instance, Lites et al. (2008) find from *Hinode* SP observations that the mean horizontal magnetic field is stronger than the mean unsigned vertical magnetic field. Using a spatial map, in the “normal mode” ( $324'' \times 164''$ ), they make magnetograms of the apparent longitudinal flux density,  $B_{\text{app}}^L$ , and apparent transverse flux density,  $B_{\text{app}}^T$ . They find a factor of 5 stronger horizontal fields: the means are  $\langle |B_{\text{app}}^L| \rangle \approx 11$  G and  $\langle B_{\text{app}}^T \rangle \approx 55$  G. A similar ratio was found in the MURaM Run C dynamo by Schüssler & Vögler (2008); see also Steiner et al. (2008). In the MURaM simulation, both small-scale, low-lying vertical loops and extended canopy-like structures are found in the line

formation region. These structures (related to flux expulsion of horizontal field) contribute to the stronger mean horizontal fields: horizontal field occupies a larger area than the narrow vertical foot points. The simulation also makes a prediction: lines with different formation heights will yield different ratios.

### 3. Measurement of the turbulent magnetic field

Whatever its source, the small-scale quiet-Sun magnetic field is turbulent. This should be taken into consideration when interpreting observations (Sanchez Almeida et al. 1996; Sánchez Almeida & Lites 2000). Consider the discrepancy between the probability distribution functions (PDFs) of the apparent vertical flux densities from the *Hinode* SP observation (discussed in the previous section) and that of  $B_z$  in MURaM dynamo Run C (see Fig. 1). For the SP observation, the PDF is peaked at  $\approx 3$  G. The simulation PDF is monotonic; there is a much greater amount of weak field than in observations. Here  $B_{\text{ave}}$  is defined as  $B_z$  averaged over the height range corresponding to  $\log \tau \in [-3.5, .1]$ : other samplings show similar PDFs. Synthetic FeI 630 nm doublet spectra are generated from the MURaM cube and used to create magnetogram signals. The PDF of the result is shown as a dashed line in Fig. 1 and begins to resemble the peaked PDF of the SP observation. With the addition of instrumental noise the PDF (dash-dotted line) becomes quite similar to that of the *Hinode* observation. The observation has a much greater amount of strong field due to the much higher  $Re_M$  of the Sun (more efficient SSD) and the presence of network elements which are not in the simulation. In any case, these considerations show that the observed peaked PDF is in fact consistent with a much greater prevalence of weak vertical magnetic field.

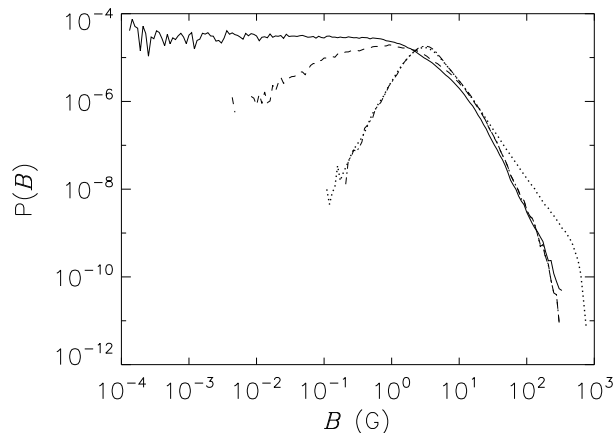


Figure 1. PDFs for magnetic field strengths and derived proxies: MURaM simulation  $B_{\text{ave}}$  (solid line), *Hinode* SP observation  $B_{\text{app}}^{\text{L}}$  (dotted line), and synthetic  $B_{\text{app}}^{\text{L}}$  from MURaM (dashed) – including noise (dot-dashed).

Vertical radiative transfer through a turbulent fluid contributes to this deformation of the PDF (Sánchez Almeida et al. 2003). In Fig. 2(a), we plot the  $z$ -components of the magnetic field and velocity for a simulation pixel with  $B_{\text{ave}} \ll B_{\text{app}}^L$ . The magnetic field undergoes a reversal above  $\tau = 1$ . The average of  $B_z$  over the line formation region is very small ( $\sim 10^{-3}$  G), but the reversal of  $B_z$  is coincident with a strong gradient in  $v_z$ . Thus, the absorption profiles from the two opposite-polarity fields are Doppler shifted with respect to each other and do not cancel. Such cancellation leads to a stronger Stokes  $V$  signal than would otherwise arise (also an asymmetric one, see Fig. 2(b)). If this statistically accounts for the differences in the PDFs, a correspondence between the strength of the velocity fluctuations along the line of sight and the synthetic magnetogram would be expected (for pixels with weak  $B_{\text{ave}}$ ). This is indeed seen in Fig. 3, which includes only pixels with  $|B_{\text{ave}}| < 0.1$  G. There exists a definite trend of stronger magnetogram signal when there are stronger Doppler shifts (velocity gradients) between the various layers of the atmosphere.

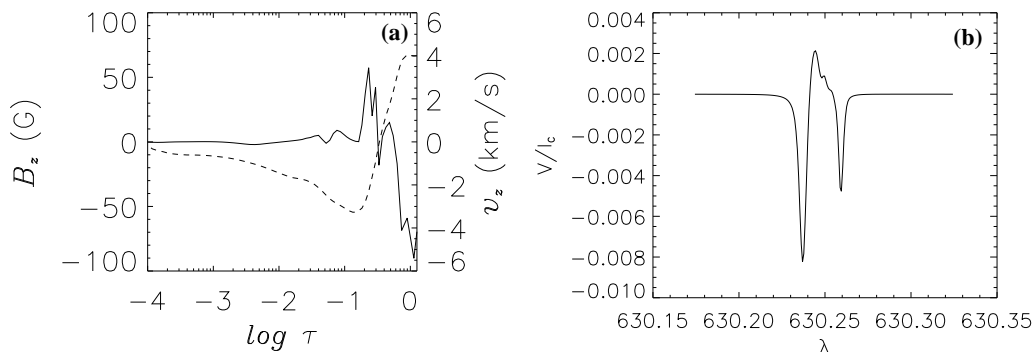


Figure 2. (a)  $B_z$  (solid line) and  $v_z$  (dashed line) versus  $\tau_{500 \text{ nm}}$ , and (b) Stokes  $V$  profile for a pixel with  $B_{\text{app}}^L = -9$  G and  $B_{\text{ave}} = -5 \cdot 10^{-3}$  G. Strong gradients can lead to  $|B_{\text{app}}^L| \gg |B_{\text{ave}}|$ .

How do gradients in the horizontal direction affect observations? Or, given that opposite-polarity vertical field inside a resolution element leads to cancellation of Stokes  $V$  signal, how can the turbulent (and hence fractal) nature of the magnetic field be used to estimate the cancellation (i.e., to get an estimate for the true unsigned vertical flux density)? Fractals are self-similar; they display power-law scaling such as in the box-counting fractal dimension: the domain is partitioned into boxes of edge length  $l$  and the number of boxes containing the fractal,  $N(l)$ , has a power-law relation,  $N(l) \propto l^{-D_f}$ , where  $D_f$  is the fractal dimension. The magnetic field, however, is more complex; for each box in a partition, there is a net flux (a magnitude) and a direction (sign), either up or down. In this case, we need to use the cancellation function,

$$\chi(l) \equiv \sum_i \left| \int_{\mathcal{A}_i(l)} B_z da \right| / \int_{\mathcal{A}} |B_z| da \quad (1)$$

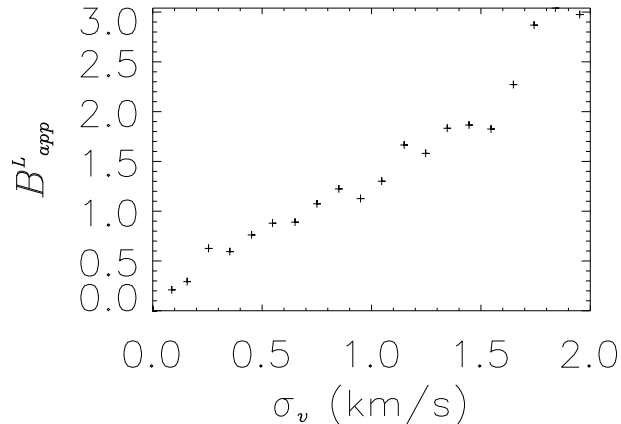


Figure 3. Average  $B_{app}^L$  versus the fluctuations of the vertical velocity along the line-of-sight,  $\sigma_v$  ( $|B_{ave}| < 0.1$  G for all pixels).

introduced by Ott et al. (1992). Simply put,  $\chi(l)$ , measures the portion of net flux remaining after averaging over boxes of length  $l$ . A fractal (self-similar) magnetic field has a power-law scaling,  $\chi(l) \sim l^{-\kappa}$ . For the magnetogram from the *Hinode* SP observation (see Fig. 4 (a)), a clear power-law scaling of the cancellation function exists over two decades of length scales down to the resolution limit at  $\approx 200$  km. Due to experience with turbulent power-laws, we can be confident that more cancellation occurs at scales down to  $\approx 20$  km or less as the power-law continues down to the resolution limit (Carbone & Bruno 1997; Sorriso-Valvo et al. 2004). It is unknown how far this power law extends, but it must stop before the magnetic dissipation scale,  $l_\eta$ . Assuming that the power law continues until dissipation sets in, we derive an estimate for the true, mean unsigned vertical magnetic field for the Sun,  $\langle |B_z| \rangle$ , defined as

$$\langle |B_z| \rangle \equiv \int_{\mathcal{A}} |B_z| da / \int_{\mathcal{A}} da. \quad (2)$$

The mean absolute value of  $B_z$  measured at resolution  $l$  is

$$\langle |B_z| \rangle_l \equiv \sum_i \left| \int_{\mathcal{A}_i(l)} B_z da \right| / \int_{\mathcal{A}} da. \quad (3)$$

Note that  $\langle |B_z| \rangle_l = \chi(l) \cdot \langle |B_z| \rangle$ . Using that there is no cancellation below the magnetic dissipation scale,  $\langle |B_z| \rangle_{l_\eta} = \langle |B_z| \rangle$ ,

$$\langle |B_z| \rangle = \langle |B_z| \rangle_l \cdot \frac{\chi(l_\eta)}{\chi(l)} = 12\text{G} \cdot \left( \frac{100 \text{ km}}{l_\eta} \right)^{0.26} \quad (4)$$

where 12 G is the 100 km result from Lites et al. (2008). We apply Kolmogorov theory to estimate  $l_\eta$  for the Sun. Assuming  $\eta \sim 10^8 \text{ cm}^2 \text{ s}^{-1}$  (Kovitya & Cram 1983), we find  $l_\eta$  to be  $\sim 80$  m. At this scale,  $\chi(l)$  must have a slope of zero and

the power-law is affected for about a decade of scales larger. There will still be some cancellation but the slope will be decreasing. Therefore, our calculation is based on a scale of 800 m in Eq. (4), giving a lower bound of  $\approx 43$  G.

An estimation for  $\langle |B_z| \rangle$  can also be obtained using the MURaM dynamo simulation. In Fig. 4 (b), we plot the cancellation at a resolution of 200 km versus  $Re_M$ . The power-law scaling can be extrapolated to the expected  $Re_M$  of the Sun  $\sim 3 \cdot 10^5$ : we estimate  $\chi(200km) \lesssim 1/5$ , which means  $\langle |B_z| \rangle \gtrsim 11 \cdot 5 \sim 55$  G. This provides qualitative agreement with Hanle estimations. Based on our estimates, the mean unsigned vertical field strength is about 40 or 50 G. As shown by Lites et al. (2008), the mean horizontal field strength is stronger. Therefore, the mean vector magnitude of the magnetic field of  $\sim 130$  G as reported by Trujillo Bueno et al. (2004) is not in contradiction with these Zeeman results.

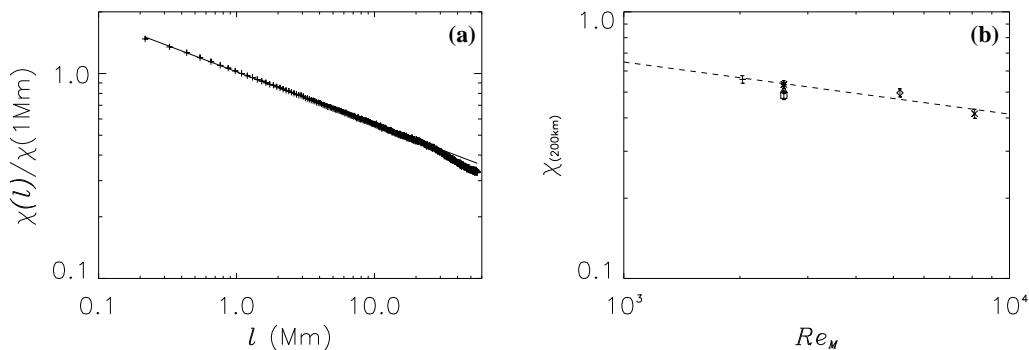


Figure 4. (a) Normalized cancellation function,  $\chi(l)/\chi(1 \text{ Mm})$ , versus scale,  $l$ , from *Hinode*  $B_{\text{app}}^L$ . The exponent of the fitted power law is  $\kappa = 0.26 \pm 0.01$ . (b) Portion of flux remaining at  $l = 200 \text{ km}$ ,  $\chi(200 \text{ km})$ , versus  $Re_M$  for MURaM dynamo. A power-law is indicated by the dashed line.

#### 4. Summary

A small-scale solar dynamo near the surface is likely. MURaM simulations show dynamo action and its properties are found to be in agreement with *Hinode* observations. The arguments against a solar small-scale dynamo, thus far, have failed. Whatever its source, the small-scale magnetic field is turbulent and fractal and this should be taken into consideration when interpreting observations: 1) the PDF of Stokes  $V$  field estimates do not accurately represent the PDF of the  $B_z$  and are consistent with a much greater prevalence of weak  $B_z$ ; 2) the multifractal self-similar pattern of the quiet-Sun photospheric magnetic field extends down to the resolution limit, 200 km. This constitutes observational evidence that the smallest scale of magnetic structuring in the photosphere is 20 km or smaller. The power law also constrains the quiet-Sun true mean unsigned vertical flux density: the lower bound,  $\approx 43$  G, is consistent with estimates based solely on numerical simulations ( $\sim 55$  G). The order of magnitude disparity between

Hanle and Zeeman-based estimates may be resolved by a proper consideration of the cancellation properties of the full vector field.

**Acknowledgments.** The authors would like to acknowledge fruitful discussions with S. Solanki, A. Pietarila, and R. Cameron. *Hinode* is a Japanese mission developed and launched by ISAS/JAXA, with NAOJ as domestic partner and NASA and STFC (UK) as international partners. It is operated by these agencies in co-operation with ESA and NSC (Norway).

## References

- Batchelor, G. K. 1950, Proceedings of the Royal Society of London. Series A, Mathematical and Physical Sciences, 201, 405
- Boldyrev, S. & Cattaneo, F. 2004, Physical Review Letters, 92, 144501
- Brandenburg, A. 2003, in Lecture Notes in Physics, Berlin Springer Verlag, Vol. 614, Turbulence and Magnetic Fields in Astrophysics, ed. E. Falgarone & T. Passot, 402–431
- Brown, B. P., Browning, M. K., Brun, A. S., Miesch, M. S., Nelson, N. J., & Toomre, J. 2007, in AIP Conference Series, Vol. 948, Unsolved Problems in Stellar Physics, ed. R. J. Stancliffe, J. Dewi, G. Houdek, & C. A. R. G. Martin, Tout, 271–278
- Carbone, V. & Bruno, R. 1997, ApJ, 488, 482
- Cattaneo, F. 1999, ApJ, 515, L39
- Cattaneo, F., Emonet, T., & Weiss, N. 2003, ApJ, 588, 1183
- Hagenaar, H. J., Schrijver, C. J., & Title, A. M. 2003, ApJ, 584, 1107
- Iskakov, A. B., Schekochihin, A. A., Cowley, S. C., McWilliams, J. C., & Proctor, M. R. E. 2007, Physical Review Letters, 98, 208501
- Kovitya, P. & Cram, L. 1983, Solar Phys., 84, 45
- Lites, B. W., Kubo, M., Socas-Navarro, H., Berger, T., Frank, Z., Shine, R., Tarbell, T., Title, A., Ichimoto, K., Katsukawa, Y., Tsuneta, S., Suematsu, Y., Shimizu, T., & Nagata, S. 2008, ApJ, 672, 1237
- Meneguzzi, M., Frisch, U., & Pouquet, A. 1981, Physical Review Letters, 47, 1060
- Monchaux, R., Berhanu, M., Bourgoïn, M., Moulin, M., Odier, P., Pinton, J.-F., Volk, R., Fauve, S., Mordant, N., Pétrélis, F., Chiffaudel, A., Daviaud, F., Dubrulle, B., Gasquet, C., Marié, L., & Ravelet, F. 2007, Physical Review Letters, 98, 044502
- Ott, E., Du, Y., Sreenivasan, K. R., Juneja, A., & Suri, A. K. 1992, Physical Review Letters, 69, 2654
- Petrovay, K. & Szakaly, G. 1993, A&A, 274, 543
- Ponty, Y., Mininni, P. D., Montgomery, D. C., Pinton, J.-F., Politano, H., & Pouquet, A. 2005, Physical Review Letters, 94, 164502
- Rogachevskii, I. & Kleeorin, N. 1997, Phys. Rev. E, 56, 417
- Sánchez Almeida, J., Emonet, T., & Cattaneo, F. 2003, ApJ, 585, 536
- Sanchez Almeida, J., Landi degl’Innocenti, E., Martinez Pillet, V., & Lites, B. W. 1996, ApJ, 466, 537
- Sánchez Almeida, J. & Lites, B. W. 2000, ApJ, 532, 1215
- Schekochihin, A. A., Haugen, N. E. L., Brandenburg, A., Cowley, S. C., Maron, J. L., & McWilliams, J. C. 2005, ApJ, 625, L115
- Schüssler, M. & Vögler, A. 2008, A&A, 481, L5
- Sorriso-Valvo, L., Carbone, V., Veltri, P., Abramenko, V. I., Noullez, A., Politano, H., Pouquet, A., & Yurchyshyn, V. 2004, Planet. Space Sci., 52, 937
- Stein, R. F., Bercik, D., & Nordlund, Å. 2003, in Astronomical Society of the Pacific Conference Series, Vol. 286, Current Theoretical Models and Future High Resolution Solar Observations: Preparing for ATST, ed. A. A. Pevtsov & H. Uitenbroek, 121–+

- Steiner, O., Rezaei, R., Schaffenberger, W., & Wedemeyer-Böhm, S. 2008, *ApJ*, 680, L85
- Title, A. M. & Schrijver, C. J. 1998, in *Astronomical Society of the Pacific Conference Series*, Vol. 154, *Cool Stars, Stellar Systems, and the Sun*, ed. R. A. Donahue & J. A. Bookbinder, 345–+
- Trujillo Bueno, J., Shchukina, N., & Asensio Ramos, A. 2004, *Nat*, 430, 326
- Vögler, A. 2003, PhD thesis, Göttingen University
- Vögler, A. & Schüssler, M. 2007, *A&A*, 465, L43
- Vögler, A., Shelyag, S., Schüssler, M., Cattaneo, F., Emonet, T., & Linde, T. 2005, *A&A*, 429, 335